Supplementary Information

$Bi_4O_5I_2$ flower/Bi_2S_3 nanorod heterojunctions for significantly enhanced photocatalytic performance

Dongfang Hou, Fan Tang, Bingbing Ma, Min Deng, Xiu-qing Qiao, Yun-Lin Liu, Dong-Sheng Li*

College of Materials and Chemical Engineering, Key Laboratory of Inorganic Nonmetallic Crystalline and Energy Conversion Materials, China Three Gorges University, Yichang, 443002, China

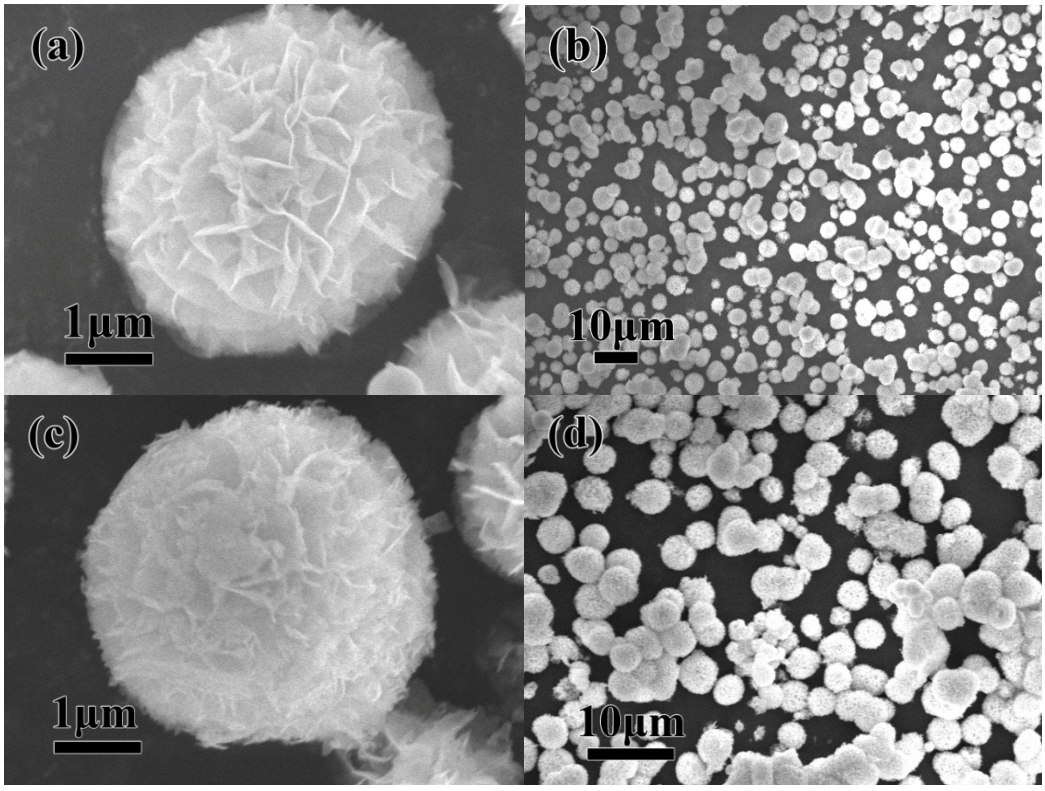

Fig. S1. Representative FESEM images of (a) and (b) the precursors, and of (c) and (d) $Bi_4O_5I_2$ microspheres after annealing

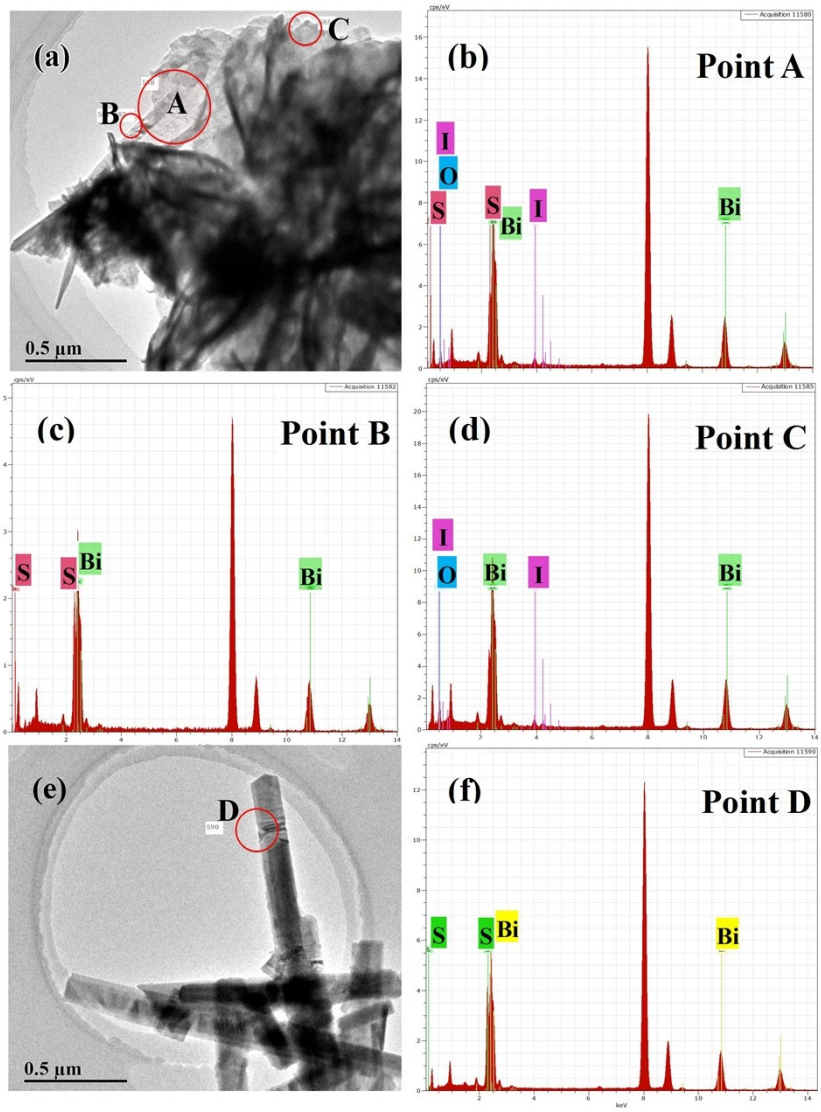

Fig. S2. TEM images and the corresponding EDX analysis of (a) BOI-S2, (b) BOI-S2-A, (c) BOI-S2-B, (d) BOI-S2-C, (e) BOI-S4, and (f) BOI-S4-D

It is easy to observe that a large number of Bi_2S_3 nanorods grow in situ from the flowers in BOI-S2, as shown in Fig. S2a. The EDX analysis of point A indicates that the existence of elements Bi, O, I, and S, which form the $Bi_4O_5I_2/Bi_2S_3$ heterostructures (Fig. S2b). Fig. S2b and 2c show the EDX results of the single nanorod (point B) and nanoflake (point C), and only Bi_2S_3 and Bi_4O_5I2 have been identified. As for BOI-S4 (Fig. S2e), it is composed of nanorods and no obvious nanoflakes are found and the corresponding EDX analysis verifies that only Bi_2S_3 exists (Fig. S2f). All these results are also based on the elements content of the BOI-S2 and BOI-S4 samples determined by EDX in Table S1.

Table S1 Elements content of the BOI-S2 and BOI-S4 samples determined by EDX

Samples	Elements	Norm. C (wt. %)	Atom. C (at. %)
BOI-S2-A	Bi	82.89	44.86
	S	10.76	37.96
	I	4,48	3.99
	O	1.86	13.18
BOI-S2-B	Bi	82.32	41.68
	S	17.68	58.32
BOI-S2-C	Bi	91.33	60.23
	I	4.64	5.04
	O	4.03	34.73
BOI-S4-D	Bi	81.71	40.67
	S	18.29	59.33

Table S2 BET surface area and pore parameters

Samples	BET surface area (m^2/g)	Mean pore diameter (nm)	Total pore volume (m^3/g)
$Bi_4O_5I_2$	18.229	39.021	0.1778
BOI-S2	21.981	30.079	0.1653
BOI-S6	7.1791	28.484	0.0511

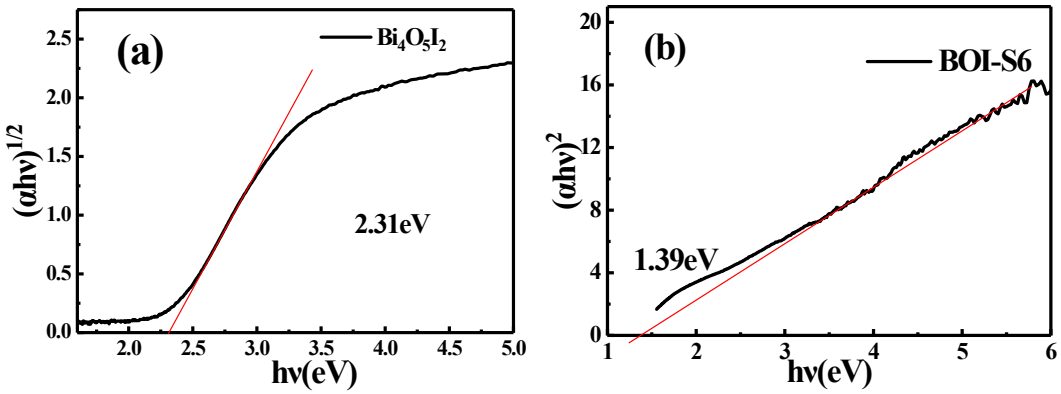

Fig. S3. The plots of transformed Kubelka–Munk function versus the energy of light for (a) $Bi4O_5I_2$ and (b) BOI (Bi_2S_3).

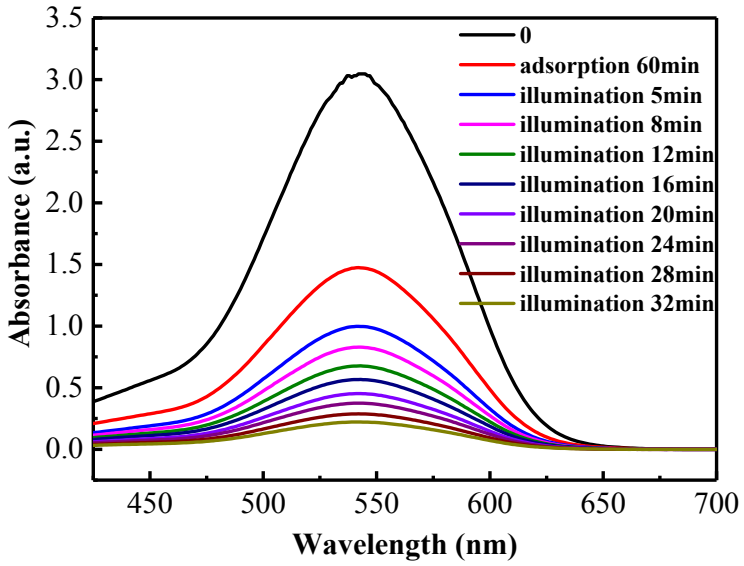

Fig. S4. Time-dependent UV-vis absorption spectra of Cr(VI) for BOI-S2

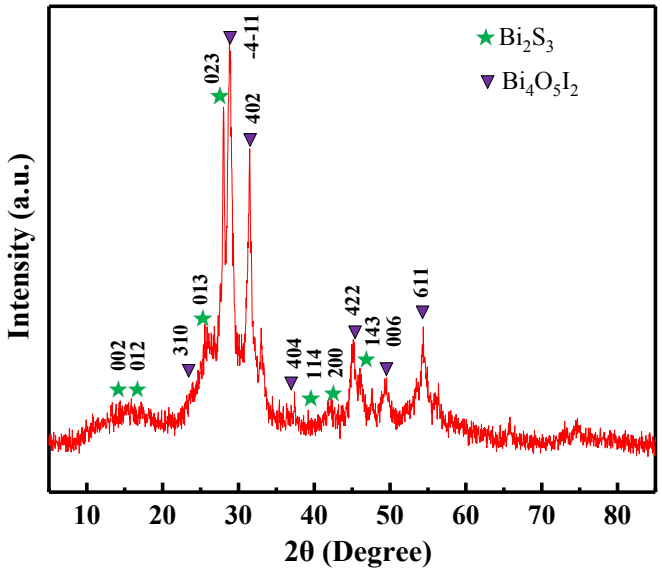

Fig. S5. XRD pattern of the $Bi_4O_5I_2/Bi_2S_3$ hetero-nanostructure (sample BOI-S2) after 5 cycles of photoreduction of Cr(VI).

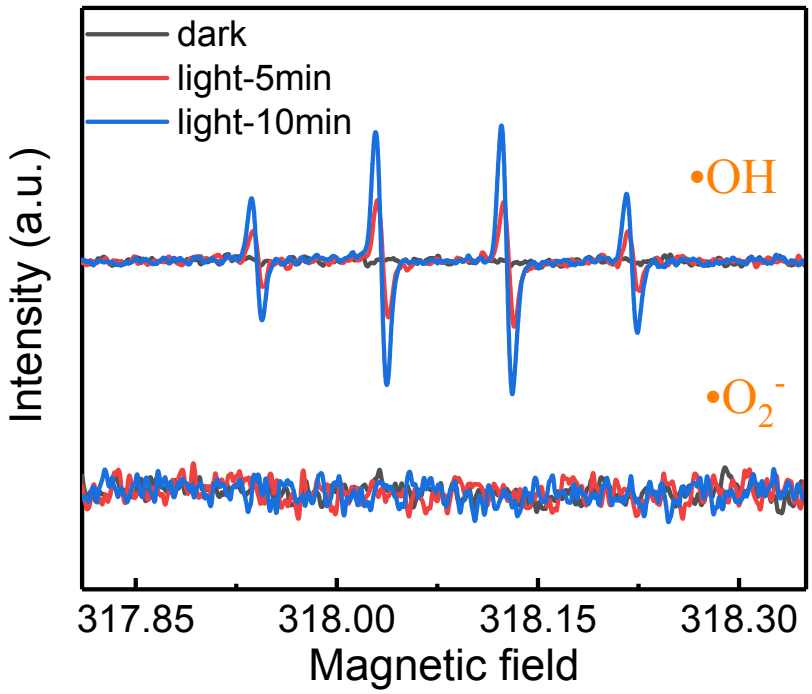

Fig. S6. DMPO spin-trapping ESR spectra recorded for •OH and $•O^{2-}$ in the dark and under visible light for BIO-2.

.